NANO LETTERS

2008
Vol. 8, No. 7
1890-1895

# Excited Excitonic States in Single-Walled Carbon Nanotubes

**Jacques Lefebvre* and Paul Finnie**

*Institute for Microstructural Sciences, National Research Council, Ottawa, Ontario K1A 0R6, Canada*

*Received February 21, 2008*

**ABSTRACT**

**Polarized photoluminescence excitation spectroscopy on individual SWNTs reveals not only the longitudinal and transverse $E_{11}$, $E_{22}$, and $E_{12}$ ground-state excitons but also excited excitonic states including the continuum. When heated, SWNTs are known to undergo a bandgap shift transition (BST), which effectively changes the nanotube dielectric environment. Here, we show that the entire spectrum of excitonic resonances blue shifts under this transition, with excited states showing larger shifts, approaching 100 meV for a 1 nm diameter nanotube. The excitonic binding energy, Coulomb self-energy correction, and dielectric shift under the BST are estimated. Analysis of this blue shift reveals the dominant effect of dielectric screening on SWNT excitonic states.**

The optical properties of semiconducting single-walled carbon nanotubes (SWNTs) are dominated by strongly bound excitons, with binding energies several hundreds of millielectronvolts. The binding energy has been estimated in a number of recent experimental reports,[1–4] with two-photon absorption providing clear experimental evidence for excitons in SWNTs.[2,3] Recently, we made an extensive study of photoluminescence (PL) excitation (PLE) spectra at the single nanotube level, and a number of absorption resonances weaker in intensity than $E_{22}$ were identified. For polarization perpendicular to the nanotube axis, the lowest transverse excitonic resonance ($E_{12}$) and related excitonic states were identified and their ($n$,$m$) dependencies determined.[5] Two longitudinal excitonic resonances directly related to the PL peak $E_{11}$ (i.e., the lowest bright exciton) were also observed. A simple inverse diameter dependence connected those resonances to $E_{11}$.

Prior to that, we discovered that, upon heating ensembles of SWNTs, the $E_{11}$ peaks undergo a bandgap shift transition (BST), a dramatic and relatively sudden blue shift of almost 30 meV.[6] Changes in PL intensity suggested that the energy $E_{22}$ changed as well. Another group reported what is essentially the same effect by increasing laser power and thus heating the SWNTs.[7] Very recently, the same effect has been observed by controllably adsorbing and desorbing ethanol molecules from the surface of SWNTs.[8] We explained the BST as occurring when molecules desorb from the nanotube surface. The change in dielectric screening due to desorption can explain the entire shift. Here, we use the BST to change the dielectric environment for individual SWNTs and track the effect of the change on all excitonic levels. The measurements reinforce our interpretation for the origin of these resonances, provide insight into the physics of the Coulomb interaction in SWNTs, and yield information about the dielectric environment.

Theory shows that excitonic energies depend strongly on the strength of the Coulomb interaction.[9–13] Experimentally, this was demonstrated early on by comparing luminescent samples in air ambient versus surfactant solution.[14] These measured energy shifts are now understood to arise from dielectric screening from the surrounding ambient. There are many reports of such shifts due to change in ambient such as those due to different solvent types,[15] different degree of bundling,[16] or different moisture levels.[17] In all cases, the observed energy shifts can be explained by the reduced Coulomb interaction (or equivalently increased dielectric screening) when a dielectric medium surrounds the nanotube, or in the case of the BST, when molecular adsorbates are present, for example, water adsorbed on the surface. Here, we use the BST as a simple way to change the Coulomb interaction and shift previously identified optical transitions.

Sample preparation is similar to our previous reports. Briefly, a $SiO_2$/Si substrate (1 $\mu$m $SiO_2$) covered with a thin Co film ($\sim$1 nm, e-beam evaporated) is patterned with trenches using photolithography, e-beam metal deposition, and wet chemistry. SWNTs are grown by chemical vapor deposition with acetylene as the carbon source. For the precise sample preparation recipe used, the yield of suspended SWNTs is low, and the likelihood of bundle formation is minimized. In addition, bundles of SWNTs have specific spectral signatures in PLE,[18,19] and no such spectral features were observed for any of the SWNTs studied here.

* Corresponding author. E-mail: jacques.lefebvre@nrc.ca.

10.1021/nl080518h CCC: $40.75 
**Published on Web 05/28/2008**

Each suspended SWNT was imaged in PL and found to be isolated, straight, and greater than 10 $\mu$m long. Some nanotubes were suspended over several supports, and on the support, the PL intensity dropped to zero. Polarized PLE spectra are obtained from imaging these individual SWNTs and integrating the PL intensity for the entire length of the nanotube for ~2 nm wavelength steps of a tunable Ti:sapphire laser (700−1050 nm). For each SWNT, a PLE spectrum is acquired for longitudinal excitation polarization (laser polarization parallel to the tube axis) and transverse excitation polarization (laser polarization perpendicular to the nanotube axis). Since the SWNTs were imaged in PL, their orientation was known, and furthermore since they were so straight, essentially pure longitudinal or transverse excitation was possible. Also, for each nanotube, a PL emission spectrum is acquired to obtain the emission wavelength. PL and PLE peak pairs ($E_{11}$, $E_{22}$) were then used for ($n$,$m$) assignment and to deduce the SWNT diameters ($d$).[20]

Each SWNT (over 20 in this work) was measured in two states. One state is "air ambient", which is the normal state for suspended SWNTs, and corresponds to the state in which the nanotube is coated with atmospheric adsorbates. The second state is the "after BST" state, for which the sample stage temperature is ramped to 450 °C under $N_2$ ambient (nitrogen flowing at 2500 sccm) and the measurement is performed while maintaining nitrogen ambient. This is the "desorbed state". Nanotubes are metastable in the "after BST" state, and the return to the "air ambient" state occurs over several hours in air. As in the original paper,[6] it was also possible to obtain spectral information intermediate to the two states, though no such data is explicitly shown here.

Many peaks are observed for each SWNT, so to enumerate them, we adopt the following labeling convention. The lowest bright excitonic peak, that is, the PL peak, is labeled $E_{11}^0$ where the superscript 0 indicates a ground state. Except where necessary, we suppress the superscript, thereby reverting to the conventional notation, $E_{11}$. The lowest transverse PLE peak, which is typically also the strongest transverse peak is labeled $E_{12}^0$, with the zero having the same meaning and being suppressed except where necessary. Likewise, the $E_{22}^0$ peak is the strongest longitudinal PLE resonance, the ground-state of the $E_{22}$ exciton, and with the subscript suppressed reverts to the conventional notation. The $E_{11}^0$ related excited states we then enumerate in order $E_{11}^1$, $E_{11}^2$, $E_{11}^3$... These states can be viewed as analogous to the familiar hydrogenic spectrum with the series $E_{11}^0$, $E_{11}^1$, $E_{11}^2$, $E_{11}^3$,... being analogues to the s, p, d, f,... states. The continuum state, an ionized $E_{11}$ exciton, or equivalently a free electron−hole pair derived from the $E_{11}$ band, is labeled $E_{11}^\infty$. The $E_{11}^\infty$ appears as a shoulder about 50 meV above $E_{11}^2$ and is distinctly visible for several species (see Supporting Information in ref 5). From previous experimental work,[2] it is expected that this continuum should appear as a shoulder and not a peak and this helps reinforce the assignment. This notation supersedes our previous,[5] provisional notation in which $E_{11}^1$ was labeled $L1$ and $E_{11}^2$ was labeled $L1^*$. The states of all other bands are readily enumerated with the general notation $E_{ij}^n$, with $i$,$j$ related to band index and $n$ related to the excitonic series.

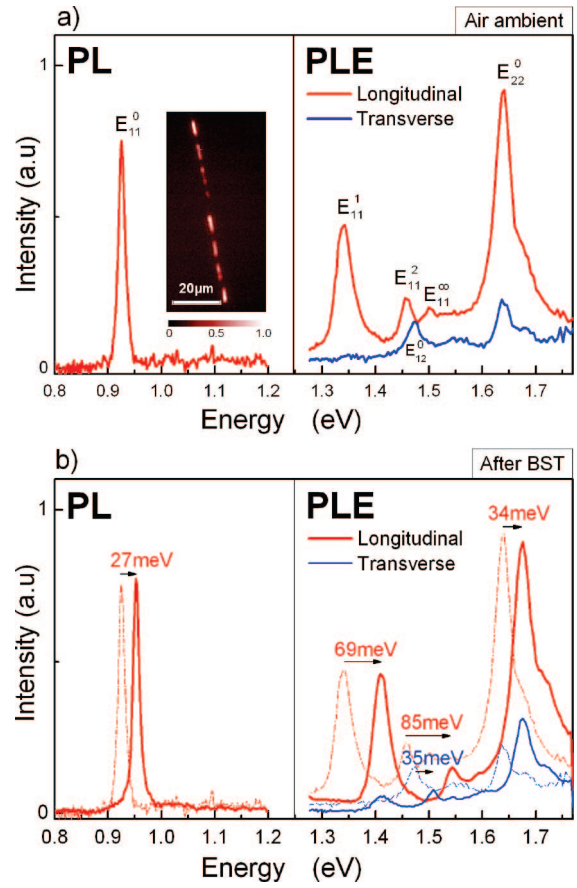


**Figure 1.** Photoluminescence (left) and polarized photoluminescence excitation (right) spectra of a ~50 $\mu$m long (10,6) SWNT. (a) Spectra in air ambient before bandgap shift transition (BST). Longitudinal excitation is plotted in red, transverse in blue. The PL peak is labeled $E_{11}^0$. The PLE peaks are labeled $E_{11}^1$, $E_{11}^2$, $E_{12}^0$, and $E_{22}^0$. The shoulder in the PLE is labeled $E_{11}^\infty$. The inset is a PL image of the single suspended SWNT. (b) Spectra before (dashed lines) and after (solid lines) the BST for the same (10,6) SWNT. The magnitude of the shift for each peak is indicated.

Figure 1 shows PL and polarized PLE data from a 50 $\mu$m long (10,6) nanotube, before and after the BST. Figure 1a shows its PL emission spectrum and the longitudinal (red) and transverse (blue) PLE spectra. All peaks are labeled as above. The inset is the spatially resolved PL image, where the dark segments arise from PL quenching where the suspended nanotube contacts the supporting silicon dioxide mesas. Figure 1b shows the PL and PLE spectra after the BST. The air ambient peaks are also shown as dotted lines, and the magnitude of the shift of each peak is labeled. The BST is a reversible process, and furthermore, there was no significant change in luminescence efficiency between the air ambient and post-BST states. All peaks are blue shifted. The excitonic ground states shift by a small amount: the $E_{11}$ emission energy is blue shifted by 27 meV, the dominant $E_{22}$ absorption resonance is blue shifted by 34 meV, and the dominant transverse resonance, $E_{12}$, blue shifts by 35 meV. By comparison, the excited states shift two to three times more, with $E_{11}^1$ shifting 69 meV and $E_{11}^2$ shifting by 85 meV. A similarly large shift is seen for $E_{11}^\infty$, although it is less

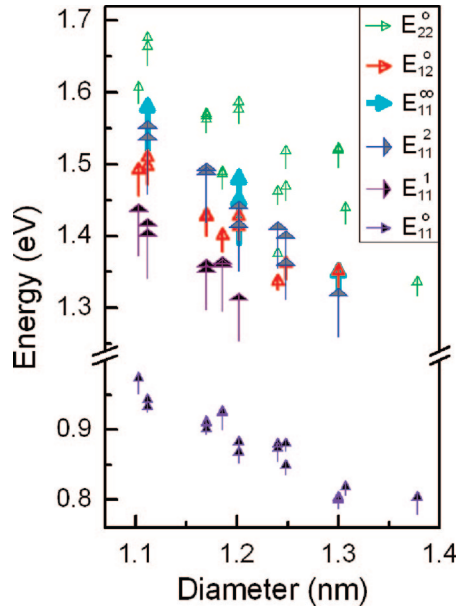


**Figure 2.** "Kataura plot" showing the energy before (arrow tail) and after (arrowhead) the BST for all investigated excitonic bands. All shift up, but with a band dependent magnitude. The mean shift for each band is indicated in the text.

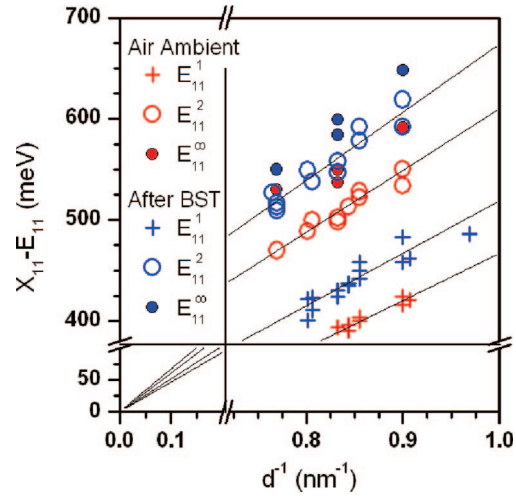


**Figure 3.** Connection between excited excitonic states $E_{11}^1$ and $E_{11}^2$ and the ground-state exciton $E_{11}^0$, for both air ambient (red) and after the BST transition (blue). The energy difference between each excited exciton resonance and the ground-state exciton PL peak is plotted versus inverse SWNT diameter. The energy difference scales linearly and extrapolates to the origin. The continuous black lines are best fit lines (see text). Although few data points are available, the continuum states $E_{11}^\infty$ are also plotted and appear to scale the same way.

clearly defined, partly because it is a shoulder not a peak, but mainly because it starts to overlap with $E_{22}$ for the (10,6). This is the case for most SWNTs under investigation here. As will be explained below from theory supported arguments, the response to dielectric change is greater for excited excitonic states compared with ground excitonic states.

This example highlights a new phenomenon of great interest from a fundamental physics perspective. In Figure 1, while $E_{11}^2$ appears at slightly lower in energy than $E_{12}$ under air ambient, it appears above $E_{12}$ after the BST. From the point of view of assigning the peaks, this provides clear evidence that they are distinct in origin. Importantly, it demonstrates that the excitonic bands can be tuned to degeneracy simply by controlling the dielectric environment surrounding the nanotube. This is especially interesting for the case of $E_{11}^\infty$ (the exciton continuum) approaching $E_{22}$ as we can expect different relaxation dynamics when the bands are pushed together or apart.

Figure 2 shows a "Kataura plot" compiling all of the data obtained in this work. Each arrow represents a given resonance and its shift under the BST for a single SWNT for which the diameter has been deduced from ($E_{11}$, $E_{22}$). The tail of an arrow marks the energy of a resonance under normal ambient conditions while the tip marks its energy after the BST. Within a given band, the arrows have globally the same, or at least very similar, magnitude. On average, for the ground states, we measured shifts of 23 ± 6 meV for $E_{11}$, 29 ± 3 meV for $E_{22}$, and 32 ± 7 meV for $E_{12}$, while for the excited states the shifts were 69 ± 4 meV for $E_{11}^1$ and 75 ± 9 meV for $E_{11}^2$. The magnitude of the shift for $E_{11}^\infty$ was similar to $E_{11}^2$, though there were too few clear data points to report a meaningful average. The scatter seen in Figure 2 originates from inhomogeneous broadening within a given ($n$,$m$) species (similar to ref 5). Because of this scatter, it was not possible to establish the existence of a chirality dependence for these shifts. The physical origin of the inhomogeneous broadening still remains to be identified. However, it is neither increased nor decreased significantly upon the BST, indicating that the adsorbates involved in the BST are not the origin of the inhomogeneous broadening.

Previously, we showed that $E_{11}^1$ and $E_{11}^2$ (then labeled *L1* and *L1**) were connected to $E_{11}$ by a simple diameter dependence.[5] A similar plot is presented in Figure 3, this time before and after the BST, and including also the position of the $E_{11}^\infty$ shoulder. The $y$ axis is calculated from the difference in energy between the excited excitonic state and the ground-state PL emission energy ($E_{11}^0$). The $x$ axis is the inverse nanotube diameter as determined from the ($n$,$m$) assignment from the PLE map. The simple linear inverse diameter dependence is preserved after the BST. In the post-BST state, the slopes are greater by 10.8 ± 0.6%. The slopes are 467 ± 5 meV•nm for $E_{11}^1$ and 610 ± 8 meV•nm for $E_{11}^2$ in the air ambient state and 519 ± 9 meV•nm for $E_{11}^1$ and 674 ± 10 meV•nm for $E_{11}^2$ after the BST. The $E_{11}^\infty$ shoulder appears to follow this linear scaling with a similar increase of slope after the BST, but the small number of data points available and their greater uncertainty makes this less clear.

A physical understanding of the origin and magnitude of this energy shift can be obtained from the excitonic picture. Excitonic energies are the result of two nearly equally important Coulombic contributions, the self-energy which increases the bandgap and the excitonic binding which decreases it. The self-energy accounts for interaction between particles of like charge. It produces a blue shift of the single particle energies without otherwise significantly altering the details of the spectrum. This is illustrated in Figure 4a where the single particle van Hove singularity illustrated in panel

(i) is shifted upward by the self-energy correction, represented by Σ, as illustrated in panel (ii). A larger Coulomb energy (i.e., a lower dielectric constant) leads to a larger self-energy correction and to a larger blue shift. The excitonic correction (X) on the other hand accounts for the attractive interaction between an electron and a hole. Its effect is quite significant in SWNTs, so as to produce both quantitative and qualitative changes to the density of states and thus to the oscillator strengths as compared with the free particle picture, as illustrated in panel (iii). The set of self-energy corrected free electron−hole bands ($E_{11}^{\infty}$, $E_{22}^{\infty}$,...) split into a series of discrete bands lower in energy than this continuum. Compared with bulk semiconductors where excitonic corrections are small, the spectral weight for SWNTs is strongly shifted from the continuum to the lowest bright exciton ($E_{11}^{0}$). The (ground state) exciton binding energy ($E_b$=$E_{11}^{\infty} - E_{11}^{0}$) increases as the strength of the Coulomb interaction increases (i.e., as the dielectric constant decreases), but its magnitude is smaller than the self-energy correction. Consequently, both corrections lead globally to a blue shift of the excitonic peaks with respect to the single-particle energy.[9] Overall, an increase of the strength of the Coulomb interaction leads to a blue shift of all spectral features.

The effect of Coulomb interaction on excitonic bands is more pronounced for bands closer to the continuum where excitonic corrections are small and self-energy dominates. This is the origin of the larger shift observed for the excited excitonic resonances ($E_{11}^{1}$ and $E_{11}^{2}$) compared with the ground-state resonances ($E_{11}$, $E_{22}$, and $E_{12}$). This reinforces the assignment of the experimentally observed peaks labeled $E_{11}^{1}$ and $E_{11}^{2}$ to the second bright exciton state and third bright exciton state, respectively.

To be more explicit in relating our experimental findings to previous theoretical work, in Figure 4b, we have replotted the theoretical results from Ando et al.,[9,23] where the energy of excitonic resonances (labeled with the current assignment) are plotted versus $U$, the strength of the Coulomb interaction, which is inversely proportional to dielectric constant. All bands increase rapidly in the small $U$ range and increase more slowly when $U$ is large. For any $U$, the excited excitonic bands ($E_{11}^{1}$, $E_{11}^{2}$,...) including the continuum $E_{11}^{\infty}$ always show the greatest slope, while $E_{11}$ and $E_{22}$ have very similar, much smaller shifts. On the other hand, $E_{12}$ with weaker excitonic corrections has intermediate shifts between $E_{11}^{\infty}$ and $E_{11}$ and $E_{22}$. Experimentally, the BST reduces the dielectric constant ($\epsilon$) or equivalently increases the Coulomb interaction strength ($U$). If Δ represents the change under the BST, the measured average shifts from smallest to largest appear in this order: $\Delta E_{11}^{0} \cong \Delta E_{22}^{0} \cong \Delta E_{12}^{0} < \Delta E_{11}^{1} < \Delta E_{11}^{2}$. This order is in agreement with Figure 4b. However, there is a discrepancy for $E_{12}$, where the theoretical model predicts a significantly greater shift. While $E_{12}^{0}$ in the experiment has the largest shifts among ground-state excitons, the magnitude of $\Delta E_{12}^{0}$ is only slightly larger than $\Delta E_{11}^{0}$ and $\Delta E_{22}^{0}$.

It seems impossible to obtain an exact match between experiment and the work of Ando et al. On the basis that

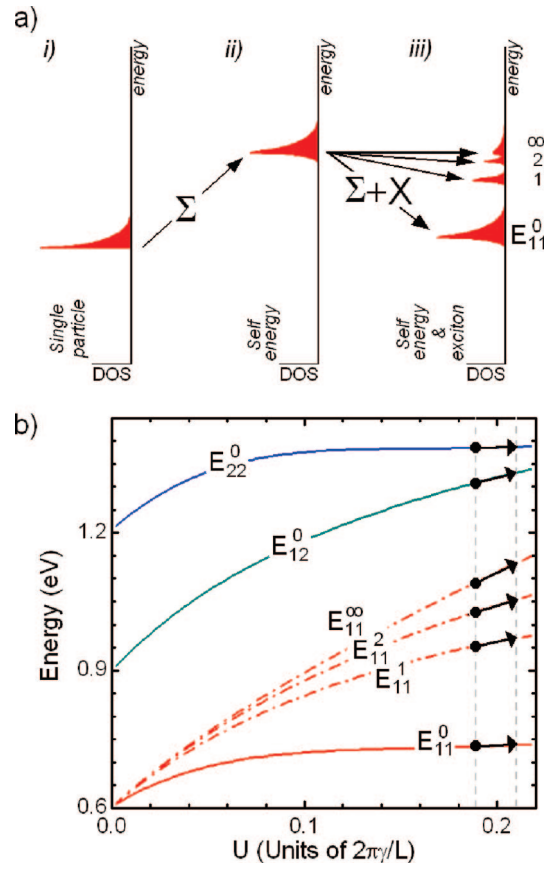


**Figure 4.** Effect of Coulomb interaction (a) on the optical spectrum of semiconducting SWNTs. Qualitative representations of the optical density of states (DOS): (i) single particle picture (that is, without Coulomb interaction), (ii) with Coulomb self-energy only, (iii) with self-energy and excitonic interactions. (b) Energy of the excitonic states as a function of the strength of the Coulomb interaction ($U$). The graph was obtained using the theoretical results from refs 9 and 23 ($\gamma_o$= 2.6 eV, $L$ = 1.24 nm, and a cutoff energy of 5).

$E_{22}^{0}$, $E_{12}^{0}$, and $E_{11}^{\infty}$ are close in energy, we found in our previous report that $U$ = 0.2 provided a fair agreement with the positions of all observed peaks.[5] However, it is not possible to quantitively account for the peak positions before and after the BST and the shift between them. As shown in Figure 4b, $E_{11}^{0}$ and $E_{22}^{0}$ depend only weakly on $U$ for $U$ = 0.2. Furthermore, while the prediction that $E_{12}^{0}$ is close to $E_{22}^{0}$ does match the expectation, the slope of the $E_{12}^{0}$ versus $U$ curve is too high to match experiment.

Although the model of Ando agrees in a general qualitative way with our data, and in this way reinforces the assignment of PLE resonances and the interpretation of the BST transition, it apparently does not agree in a rigorous, quantitative way. One possible explanation is that modeling the nanotube as embedded in an environment parametrized by a single dielectric constant is overly simple. For example, it may be more accurate to have a surface dielectric constant to account for screening at or near the surface of the nanotube and a bulk dielectric constant to account for distances further away. A surface dielectric constant would be expected to change drastically during the BST. Furthermore, since excited excitonic states are more delocalized than ground states, they are likely to sample an inhomogeneous dielectric environ-

ment differently. In any case, it is likely that the calculations were never intended to be accurate to the level of precision which is now accessible to experiment.

The exciton binding energy is a quantity of special interest. The $E_{11}$ exciton binding energy is defined as $E_B = E_{11}^{\infty} - E_{11}^{0}$. The continuum $E_{11}^{\infty}$ is not very precisely measured here but in general was ~50 meV above $E_{11}^{2}$. We thus get $E_B \cong E_{11}^{2} - E_{11}^{0} + 50$ meV. Using the linear relationships derived from Figure 3, $E_B \cong 725$ meV for a 1 nm diameter SWNT. This number and the inverse diameter scaling agree well with theoretical prediction. Capaz et al. reported 672 meV·nm/$d$ to first order for $E_b$ using $\varepsilon = 1.846$.[21] Jiang et al. predict a binding energy of 1 eV for a (6,5) with $\varepsilon \cong 1$, which when scaled for diameter would then correspond to ~800 meV for a 1 nm nanotube.[12] Both models predict a chirality dependence for the binding energy which was not observed. Theoretically, however, the chirality dependence becomes weak for larger diameter nanotubes and appears to be within the scatter of our experimental data.

These values of exciton binding energy are significantly larger than those deduced from transient absorption,[1] two-photon luminescence,[2,3] Raman scattering,[4] or photocurrent spectroscopy,[22] which fall in the range of 350 to 500 meV for a 1 nm diameter nanotube. The origin of this difference is likely to be the stronger dielectric screening in those cases, arising from the surfactant solution or from the $SiO_2$ substrate.

It is possible to estimate the change of the dielectric constant during the BST. Pereibenos et al. proposed a power law scaling $E_B \propto \epsilon^{-\alpha}$ of the exciton binding energy with dielectric constant.[11] Under power law scaling, the relative change in the exciton binding energy is proportional to the relative change in dielectric constant, with the constant of proportionality being the scaling exponent (i.e., $\Delta E_B/E_B = -\alpha\Delta\epsilon/\epsilon$). Pereibenos et al. predict that $\alpha = 1.4$. Using the $10.8 \pm 0.6\%$ change of in the exciton binding energy ($E_B$) in the present experiment, we calculate a corresponding $7.7 \pm 0.4\%$ reduction in the dielectric constant ($\varepsilon$) after the BST. Other calculations suggest different scaling exponents, for example, the results in Figure 3 of Ando are better fit with $\alpha \cong 1$ which would increase this value to $10.8 \pm 0.6\%$. By estimating $E_B$ for nanotubes in solution at approximately 425 meV and using the estimated post-BST exciton binding energy at 725 meV, the same argument for $\alpha = 1.4$ predicts an approximately 30% difference in dielectric constant for nanotubes in solution as compared with post-BST nanotubes.

It is also of interest to estimate the magnitude of the self-energy correction ($\Sigma$). If we assume, similar to the exciton binding energy, that the magnitude of the self-energy correction scales as a power law (i.e., $\Sigma \propto \epsilon^{-\beta}$), we obtain a direct relationship between the two quantities, $\Delta E_B/E_B = \alpha/\beta \cdot \Delta\Sigma/\Sigma$. To leading order, it was proposed that the scaling exponent for $\Sigma$ should be $\beta = 1$,[17] a scaling consistent with the classical Coulomb interaction energy. With the relative change in the exciton binding energy $\Delta E_B/E_B = 10.8 \pm 0.6\%$, the change in self-energy $\Delta\Sigma = \Delta E_{11}^{\infty} \cong \Delta E_{11}^{2} = 75 \pm 9$ meV·nm/$d$ (since $E_{11}^{2}$ is close to the continuum and is spectrally well defined, we use it instead of $E_{11}^{\infty}$), and the scaling exponents $\alpha = 1.4$ and $\beta$=1, the self-energy term is estimated to $\Sigma = 980 \pm 170$ meV·nm/$d$. This value is larger than the exciton binding energy of $E_B \cong 725$ meV for a 1 nm diameter nanotube. Presumably, the nanotubes measured after the BST would be closest to the state with $\varepsilon = 1$.

This argument above does not require knowledge of the actual value of the dielectric constant but rather depends on the scaling relationship and its exponent. There is no experimental measurement available yet for either $\alpha$ or $\beta$. It is interesting that for $\alpha = \beta$ (e.g., for classical Coulomb scaling in which $\alpha = \beta = 1$) the calculated self-energy and exciton binding energy are the same here, to within experimental precision. However, it is expected that the exciton binding energy should be less than the self-energy term, which is the case for $\alpha = 1.4$ and $\beta = 1$, for example.

In this work, we have shown how ground state ($E_{11}$, $E_{22}$, and $E_{12}$) and excited state ($E_{11}^{1}$, $E_{11}^{2}$, and $E_{11}^{\infty}$) optical resonances of individual SWNTs of diameters ranging from $d = 1.1$ nm to 1.4 nm blue shift under the BST, a transition understood to occur when atmospheric adsorbates are desorbed. The ground states shift by ~30 meV while the excited states shift by a factor of 2−3 or more. With the assumption that the BST blue shift is caused solely by a change in dielectric constant, we conclude that the shifts are in qualitative agreement with theoretical prediction. The exciton binding energy after the BST, that is, for $\varepsilon$ closest to 1, is 725 meV for 1 nm diameter nanotube, and this number scales inversely with diameter. This is an 11% shift compared with SWNTs in air ambient. Scaling arguments with plausible values of scaling exponents suggest that the change in dielectric constant under the BST is approximately 8% and that the self-energy correction to the single particle picture is approximately 1 eV.

Since excitonic peak positions can be tuned widely, opportunities arise both for fundamental studies as well as potential applications. Given the larger spectral shift of excited states, SWNT sensors based on optical absorption into excited excitonic states can be expected to have greater sensitivity than those based on excitonic ground states. Furthermore, the PLE spectrum of excitonic states is a kind of fingerprint of the SWNT dielectric environment.

While this experiment provides information on optical properties of SWNTs, it also has implications for electronic transport in SWNTs and the understanding of SWNT field effect transistors (FETs). Charge transport occurs through the continuum band, demonstrated here to be very sensitive to changes in the Coulomb interaction strength. In SWNT devices, the dielectric environment changes drastically along the length of the nanotube, as there are, typically, segments of the SWNT on oxide or metal or even suspended in air. Because of the self-energy correction, the transport bandgap should be strongly modulated in SWNT FETs. Furthermore, since the continuum band blue shifts markedly through the BST, transport characteristics of nanotube FETs should be sensitive to the BST.

**Acknowledgment.** We are grateful for the assistance of IMS staff for sample preparation including D. G. Austing, P. Chow-Chong, H. Tran, and P. Marshall.

## References


(1) Ma, Y.-Z.; Valkunas, L.; Bachilo, S. M.; Fleming, G. R. *J. Phys. Chem B* **2004**, *109*, 15671.
(2) Wang, F.; Dukovic, G.; Brus, L. E.; Heinz, T. F. *Science* **2005**, *308*, 838.
(3) Maultzsch, J.; Pomraenke, R.; Reich, S.; Chang, E.; Prezzi, D.; Ruini, A.; Molinari, E.; Strano, M.; Thomsen, C.; Lienau, C. *Phys. Rev. B* **2005**, *72*, 241402.
(4) Wang, Z.; Pedrosa, H.; Krauss, T.; Rothberg, L. *Phys. Rev. Lett.* **2006**, *96*, 047403.
(5) Lefebvre, J.; Finnie, P. *Phys. Rev. Lett.* **2007**, *98*, 167406.
(6) Finnie, P.; Homma, Y.; Lefebvre, J. *Phys. Rev. Lett.* **2005**, *94*, 247401.
(7) Milkie, D. E.; Staii, C; Paulson, S; Hindman, E; Johnson, A. T.; Kikkawa, J *Nano Lett.* **2005**, *5*, 1135.
(8) Chiashi, S.; Hanashima, T.; Homma, Y. Program and Abstracts, The 9th International Conference on Atomically Controlled Surfaces, Interfaces and Nanostructures (ACSIN-9). **2007**, 84.
(9) Ando, T. *J. Phys. Soc. Jpn.* **1997**, *66*, 1066.
(10) Pedersen, T. G. *Phys. Rev. B* **2003**, *67*, 073401.
(11) Pereibenos, V.; Tersoff, J.; Avouris, P. *Phys. Rev. Lett.* **2004**, *92*, 257402.
(12) Jiang, J.; Saito, R.; Samsonidze, Ge. G.; Jorio, A.; Chou, S. G.; Dresselhaus, G.; Dresselhaus, M. S. *Phys. Rev. B* **2007**, *75*, 035407.
(13) Miyauchi, Y.; Saito, R.; Sato, K.; Ohno, Y.; Iwasaki, S.; Mizutani, T.; Jiang, J.; Maruyama, S. *Chem. Phys. Lett.* **2007**, *442*, 394.
(14) Lefebvre, J.; Fraser, J. M.; Homma, Y.; Finnie, P. *Appl. Phys. A: Mater. Sci.* **2004**, *78*, 1107.
(15) Ohno, Y; Iwasaki, S; Murakami, Y; Kishimoto, S; Maruyama, S; Mizutani, T, http://arxiv.org/abs/0704.1018, 2007..
(16) Wang, F; Sfeir, M. Y; Huang, L.; Huang, X. M. H.; Wu, Y; Kim, J.; Hone, J.; O'Brien, S.; Brus, L. E.; Heinz, T. F. *Phys. Rev. Lett.* **2006**, *96*, 167401.
(17) Walsh, A. G.; Vamivakas, A. N.; Yin, Y.; Cronin, S. B.; Ünlü, M. S.; Goldberg, B. B.; Swan, A. K. *Nano Lett.* **2007**, *7*, 1485.
(18) Torrens, O. N.; Milkie, D. E.; Zheng, M.; Kikkawa, J. M. *Nano Lett.* **2006**, *6*, 2864.
(19) Tan, P. H.; Rozhin, A. G.; Hasan, T.; Hu, P.; Scardaci, V.; Milne, W. I.; Ferrari, A. C. *Phys. Rev. Lett.* **2007**, *99*, 137402.
(20) Weisman, R. B.; Bachilo, S. M. *Nano Lett.* **2003**, *3*, 1235.
(21) Capaz, R. B.; Spataru, C. D.; Ismail-Beigi, S.; Louie, S. G. *Phys. Rev. B* **2006**, *74*, 121401.
(22) Mohite, A. D.; Gopinath, P.; Shah, H. M.; Alphenaar, B. W. *Nano Lett.* **2008**, *8*, 142.
(23) Uryu, S.; Ando, T. *Phys. Rev. B* **2006**, *74*, 155411.


NL080518H